

CEBAF Program Advisory Committee Eight Cover Sheet

This proposal must be received by close of business on Thursday, April 14, 1994 at:

CEBAF

User Liaison Office, Mail Stop 12 B

12000 Jefferson Avenue

Newport News, VA 23606

Proposal Title

Measurement of Photoproton Polarization
in the $H(\gamma, p^+) \pi^0$ Reaction

Contact Person

Name: Ronald Gilman

Institution: Rutgers University

Address: P.O. Box 849

Address:

City, State ZIP/Country: Piscataway, NJ 08855-0849 USA

Phone: (908) 932-5489 FAX: (908) 932-4343

E-Mail → Internet: GILMAN@RUTHEP.RUTGERS.EDU

Experimental Hall: A

Total Days Requested for Approval: 2

Minimum and Maximum Beam Energies (GeV): 0.8 to 4.0

Minimum and Maximum Beam Currents (μ Amps): 0.1 to 50.0

CEBAF Use Only

Receipt Date: 4/14/94

PR 94-012

By:

by Smith

HAZARD IDENTIFICATION CHECKLIST

CEBAF Experiment: ^{Measurement of} Proposed Photoproton Polarization in the $H(p,p^0)$ Reaction Date: 4/11/94

Check all items for which there is an anticipated need—do not check items that are part of the CEBAF standard experiment (HRSE, HRSH, CLAS, HMS, SOS in standard configurations).

Cryogenics <input type="checkbox"/> beamline magnets <input type="checkbox"/> analysis magnets <input checked="" type="checkbox"/> target <i>standard cell A</i> <input type="checkbox"/> drift chambers <input type="checkbox"/> other	Electrical Equipment <input type="checkbox"/> cryo/electrical devices <input type="checkbox"/> capacitor banks <input type="checkbox"/> high voltage <input type="checkbox"/> exposed equipment	Radioactive/Hazardous Materials List any radioactive or hazardous/toxic materials planned for use: _____ _____
Pressure Vessels <input type="checkbox"/> inside diameter <input type="checkbox"/> operating pressure <input type="checkbox"/> window material <input type="checkbox"/> window thickness	Flammable Gas or Liquids (incl. target) type: _____ flow rate: _____ capacity: _____	Other Target Materials <input type="checkbox"/> Beryllium (Be) <input type="checkbox"/> Lithium (Li) <input type="checkbox"/> Mercury (Hg) <input type="checkbox"/> Lead (Pb) <input type="checkbox"/> Tungsten (W) <input type="checkbox"/> Uranium (U) <input type="checkbox"/> Other (list below) _____ _____
Vacuum Vessels <input type="checkbox"/> inside diameter <input type="checkbox"/> operating pressure <input type="checkbox"/> window material <input type="checkbox"/> window thickness	Radioactive Sources <input type="checkbox"/> permanent installation <input type="checkbox"/> temporary use type: _____ strength: _____	Large Mech. Structure/System <input type="checkbox"/> lifting devices <input type="checkbox"/> motion controllers <input type="checkbox"/> scaffolding or elevated platforms <input type="checkbox"/> other
Lasers type: _____ wattage: _____ class: _____ Installation <input type="checkbox"/> permanent <input type="checkbox"/> temporary Use <input type="checkbox"/> calibration <input type="checkbox"/> alignment	Hazardous Materials <input type="checkbox"/> cyanide plating materials <input type="checkbox"/> scintillation oil (from) <input type="checkbox"/> PCBs <input type="checkbox"/> methane <input type="checkbox"/> TMAE <input type="checkbox"/> TEA <input type="checkbox"/> photographic developers <input type="checkbox"/> other (list below) _____ _____ _____	Notes: <u>photon radiator will</u> <u>be used (Cu) in</u> <u>beamline</u> _____ _____ _____

**Measurement of Photoproton Polarization
in the $H(\gamma, \bar{p})\pi^0$ Reaction**

D. F. Geesaman, R. J. Holt (Spokesperson),
H. E. Jackson, C. E. Jones, T.-S. H. Lee, D. Potterveld, B. Zeidman
ARGONNE NATIONAL LABORATORY
B. Filippone, R. D. McKeown
CALIFORNIA INSTITUTE OF TECHNOLOGY
J. Gomez, J. LeRose, R. Michaels, S. Nanda, A. Saha
CONTINUOUS ELECTRON BEAM ACCELERATOR FACILITY
J. E. Belz, E. Kinney
UNIVERSITY OF COLORADO
P. Rutt
UNIVERSITY OF GEORGIA AND RUTGERS UNIVERSITY
D. Beck, A. M. Nathan, R. M. Laszewski, S. E. Williamson
UNIVERSITY OF ILLINOIS
G. G. Petratos
KENT STATE UNIVERSITY
E. Beise, N. Chant, P. Markowitz, P. Roos
UNIVERSITY OF MARYLAND
R. Milner
MASSACHUSETTS INSTITUTE OF TECHNOLOGY
K. P. Coulter
UNIVERSITY OF MICHIGAN
R. E. Segel
NORTHWESTERN UNIVERSITY
P. Ulmer
OLD DOMINION UNIVERSITY
L. Bimbot
IPN ORSAY AND RUTGERS UNIVERSITY
G. Adams, J. Napolitano, B. Wojtsekhowski
RENSSELAER POLYTECHNIC INSTITUTE
D. P. Beatty, E. Brash, R. Gilman (Spokesperson), C. Glashausser
G. Kumbartzki, R. Ransome
RUTGERS UNIVERSITY
L. Auerbach, J. Martoff, Z.-E. Meziani
TEMPLE UNIVERSITY

I. ABSTRACT

We propose to measure photoproton cross sections and polarizations in the reaction $H(\gamma, \vec{p})\pi^0$ for photon energies from 0.8 to 4.0 GeV at center of mass angles between 45° and 90° . Existing cross section data for $H(\gamma, \pi^+)n$ exhibit an energy dependence near $\theta_{cm} = 90^\circ$ consistent with asymptotic scaling for photon energies above about 2 GeV. However, existing data sets for the $H(\gamma, p)\pi^0$ cross sections are in disagreement with one another. Moreover, no polarization data exist for any exclusive photoreactions at high energy. Since there are no Landshoff terms in photoreactions, the combination of high energy differential cross section and polarization measurements for a simple photoreaction involving spin would provide the most stringent tests to date for asymptotic scaling in exclusive processes.

II. INTRODUCTION

Two tests of asymptotic QCD in exclusive nuclear reactions have been proposed: (i) whether the reaction obeys the constituent counting rules and (ii) whether hadron helicity is conserved. Most exclusive reactions appear to obey the constituent counting rules at high energy and momentum transfer. However, attempts to observe hadron helicity conservation are believed to be obscured by the presence of Landshoff amplitudes – see Fig. 1 – which appear in hadron-hadron collisions but not in photoreactions. Here, we propose to measure, for the first time, one of the simplest exclusive photoreactions in an energy region where the constituent counting rules appear to work [1] – see Fig. 2. The $H(\gamma, \vec{p})\pi^0$ reaction is an excellent case for testing hadron helicity conservation, not only because it involves a relatively small number of constituents and only two helicity amplitudes, but also because it is one the most technically feasible experiments.

In this proposal, we first summarize the search for hadron helicity conservation in exclusive processes. We then describe some predictions for the $H(\gamma, \vec{p})\pi^0$ reaction, from both a scaling picture and a meson + nucleon picture. Finally, we present the proposed experiment and its technical merits.

III. SCIENTIFIC MOTIVATION

Hadron helicity conservation arises from the helicity conservation expected in photon interactions with individual quarks. To the extent that the individual quark mass is much smaller than the photon energy, quark helicity is conserved in high energy processes. Also, in a reaction which occurs at short distances, the small transverse momentum of quarks in a hadron will lead to a small or negligible amount of angular momentum in the direction of the hadron's motion. Thus, quark helicity conservation leads to hadron helicity conservation.

During the past two decades, an extensive search for hadron helicity conservation has been performed for pp elastic scattering. It is known [2] that pp elastic cross sections fall as $d\sigma/dt \approx s^{-10}$ at constant center of mass angle for $s > 15 \text{ GeV}^2$, equivalent to an incident kinetic energy of about 6 GeV, and $-t > 2.5 \text{ GeV}^2$, equivalent to a center of mass scattering angle of almost 60° at the limiting value of s . This is generally accepted as evidence for scaling since the exponent is believed to be 10 from constituent counting rules. However, the presence of oscillations about the s^{-10} dependence shown in Fig. 3(a) as well as non-zero polarizations have cast considerable doubt upon the interpretation of the data. The oscillations are believed to arise from a hard interaction amplitude interfering with a Landshoff term. The curve in Fig. 3(a), from Ref. [3], utilizes this explanation.

Polarization transfer experiments indicate that in the same energy region where the oscillations in the cross section are observed, A_{nn} also has a large energy dependence [4]. In fact, the data can be explained readily by the same model [3] as is shown in Fig. 3(b). If hadron helicity were conserved, A_{nn} is expected to be about $1/3$ [3,4,5].

Analyzing power measurements [6] have been performed up to an incident proton momentum of $28 \text{ GeV}/c$, corresponding to $s = 54.4 \text{ GeV}^2$. These data, shown in Fig. 4, indicate that for p_\perp^2 from about 3 to $7 (\text{GeV}/c)^2$, corresponding to $-t$ ranging from 3 to $9 (\text{GeV}/c)^2$, the analyzing power increases approximately linearly with p_\perp^2 from about 0.0 to 0.2, with small uncertainties. This is in contrast to the scaling prediction of an analyzing power of zero.

It is now believed that exclusive proton-proton scattering is probably not a good case for exploration of the onset of scaling. Not only are five helicity amplitudes involved in the process, but Landshoff or long-distance quark-quark scattering terms are believed to be responsible for non-zero polarizations. The independent quark scattering Landshoff amplitude [3] – see Fig. 1 – is expected to fall off with energy at about the same rate as the short-range hard-scattering asymptotic amplitude. Since the Landshoff amplitude can induce polarizations at high momentum transfer, pp elastic scattering can generally be expected to show some polarization effects. While the relative contributions of Landshoff and asymptotic amplitudes are difficult to evaluate from theory, fits [3] to pp scattering data indicate that the Landshoff amplitude is important.

In contrast, there are no Landshoff terms in reactions such as pion photo-production. The result is an experiment for which the theory is clearer, and interpretation of the data can be more definitive. The scaling prediction for the cross sections is $d\sigma/dt \sim s^{-7}$ for constant angle in the center of mass. The scaling prediction for the polarization is 0 at all angles, from helicity conservation.

A first attempt [7] to extend the meson-exchange model into the “scaling” region is shown in Fig. 5. Here, the classical meson exchange calculation has been modified by changing the $\pi - NN$ form factor from a monopole to a dipole in the high energy regime. This has the equivalent effect of accounting for the quark substructure of the proton which is probed by the high energy photon. The result gives a reasonable prediction for the fall-off of the $H(\gamma, \pi^+)n$ cross section and predicts a small polarization for the $H(\gamma, \vec{p})\pi^0$ reaction, as shown in Fig. 5(a). This very preliminary calculation does not include nucleon resonances above 500 MeV and has a rather simple final state interaction. The predicted angular distribution shown in Fig. 5(b) has nearly a $\sin(2\theta)$ dependence and further illustrates the need for measurements of the photoproton polarization at more than one angle.

In general, it is expected that the onset of scaling requires large values for all the Mandelstam variables, s , t , and u [8]. Thus, for fixed incident energy, the physical picture may change from scaling behavior near 90°_{cm} to nonscaling behavior at the forward and backward angles. This has been described previously with respect to the scaling behavior of the pp differential cross sections.

IV. PROPOSED MEASUREMENTS

We propose to measure $H(\gamma, \vec{p})\pi^0$ at 45°_{cm} , 60°_{cm} , and 90°_{cm} for photon energies from 0.8 to 4.0 GeV, in steps of 0.8 GeV. The proposed kinematics are shown in Table 1. We will use the focal plane polarimeter in the Hall A HRS hadron spectrometer to perform this measurement. The HRS electron spectrometer will be used to tag electrons from ep elastic scattering in order to remove these events from the analysis.

The choice of angles is both the minimum needed to test scaling in the reaction and the maximum allowed by practical considerations. The forward angle is limited by the minimum angle of the HRS hadron spectrometer, while the backward angle is limited by the relatively high rate of ep elastic scattering. Cross section data for $H(\gamma, p)\pi^0$ are sparse and contradictory. We will repeat the cross section measurements at the same energies and angles as the polarization measurements as a check of previous data. The motivation for the choice of beam energies was compatibility with the expected operation of the CEBAF accelerator and the most convenient energy changes.

V. EXPERIMENTAL TECHNIQUE

The basic experimental technique is as follows. The electron beam strikes a radiator, producing a 0° bremsstrahlung photon beam with maximum energy essentially equal to the electron kinetic energy. The target, located downstream of

the radiator, is irradiated by both the photons and electrons. Outgoing protons from the $H(\gamma, p)\pi^0$ reaction, as well as background particles, are detected in the Hall A HRS spectrometer containing the focal plane polarimeter. Electrons from the concurrent ep elastic scattering are detected in the other Hall A HRS spectrometer which is located at the conjugate angle for ep elastic scattering from the target.

Note that, because the $H(\gamma, p)\pi^0$ reaction has only two bodies in either the initial or final state, the angle and energy measurement of the outgoing proton completely determines the energy and momentum vector of the π^0 , as well as the incident photon energy. This kinematic fact, coupled to our measuring only protons from near the endpoint of the bremsstrahlung spectrum, allows the experiment to be run with the large nonmonochromatic bremsstrahlung photon flux.

The radiator will be 6% of a radiation length of Cu. The Cu will be placed in the scattering chamber at least 30 cm upstream of the pivot, so that the spectrometer does not view it directly at our most forward angles. Energy loss in the Cu is about 90 watts. The radiator assembly will be the same as that planned for approved Experiment 89-019. The radiator does contribute to background in the Hall both through increased production of low energy neutrons and increased production of high energy pions that can penetrate thick shielding. Based on estimates [9] of backgrounds at 4 GeV from these processes, the radiator will contribute perhaps a few kHz of singles rate to each scintillator in the detector stack, leading to almost no triggers.

Another consideration is the total amount of energy deposited in the Hall or beam dump tunnel, rather than in the beam dump itself. Since we plan to run a total target thickness (including the 2.0% hydrogen target) of about 8.0% at highest energy and current of 4.0 GeV and 50 μA , we are below the Hall A design limits of 3.0% target at 4.0 GeV and 200 μA . This issue has been studied in most detail for Hall C experiment 89-012 [10]. Power deposited in the beam dump tunnel but outside the dump does not appear to be a problem. Extrapolating to the current experiment, we estimate that less than 1 kW of power will be deposited in the tunnel and outside of the dump; this is significantly less than is estimated for experiment 89-012. Of more concern is the power deposited in the Hall, from interactions in the thick target. Based on the simple estimate above and those of ref. [10], we are approaching power limits for the 4 GeV measurements. It may be necessary to either request some additional time for these measurements, or to install local shielding near the target to reduce neutron skyshine. This issue will be understood much better after measurements have been made in Hall C for experiment 89-012. Since the experimental time is determined by luminosity

limits rather than count rate limits, we would choose to run all but the lowest energy kinematics at a higher luminosity at the time of the experiment if that were to prove feasible.

The Hall A cryotarget is designed for heat loads up to 1 kW, much greater than the 200 W load for this experiment. The cryotarget, required by almost all approved Hall A experiments, should be available. In fact, because of the very high counting rates and low requirements on beam and target power and monitoring, this may well be a desirable commissioning experiment for the cryotarget. At this heat load, the average temperature change of the target liquid will be less than 1 K, so density fluctuations should be negligible. The luminosity will be monitored with the singles rates in the electron spectrometer, in as much as this spectrometer will be used to monitor the $ep \rightarrow ep$ reaction, for which the cross sections can be estimated. Also, density fluctuations do not affect the polarization measurement.

The HRS spectrometers will be used in their standard configuration. The major source of background in this experiment is protons from ep elastic scattering in the LH2 target, which show up in the detectors at nearly the same momentum as protons from the $H(\gamma, p)\pi^0$ reaction. The rates for this background process are shown in Table 1 along with the desired $H(\gamma, \bar{p})\pi^0$ counting rates.

Background will be subtracted in three ways. First, as a result of the kinematics, the elastic proton peak is higher in energy than the bremsstrahlung end point protons from $H(\gamma, p)\pi^0$, and these protons may be removed by a simple momentum cut. Except for radiative effects, all of the elastic protons could be removed by this technique. Second, the electron HRS will be tuned to detect the elastically scattered electrons from the target. Electrons, detected in coincidence with protons in the hadron HRS, will be used to “veto”, in software, the ep scattering events. (The trigger in Hall A is sufficiently flexible to read out the proton arm in singles mode, and the electron arm only if there is a coincident proton. This is advantageous because it may be difficult to determine in hardware if the electron arm event is an electron or a background particle.) The proton rates in the hadron spectrometer for these processes are shown in Table 1. Clearly, the rates are not so large as to give rise to significant accidental vetoes of the real protons. The rejection efficiency was determined by a Monte Carlo simulation of the process and was found to be greater than 90% in all cases. Clearly, the highest background rates occur for the large angle case. Third, any remaining background events can be readily subtracted by measuring the yield with radiator in and out.

A second source of background arises from π^+ 's from the $H(\gamma, \pi^+)n$ reaction. This background shows up at close to the same momentum as the protons of

interest at 90°_{cm} above a photon energy of 2 GeV. At more forward angles or lower energies, the π^+ are at least 5% lower in momentum. Although the π^+ will be removed from the spectrum with an efficiency of 99% by the aerogel Čerenkov counter, we have also estimated the rate of this reaction. After the veto, the π^+ contamination becomes negligible, i.e. $\leq 1\%$.

Background particles also come from the Al endcaps of the target. These will not be a problem, as the spectrometer design indicates 1 mm resolution in transverse position at the target. At our most forward angle, a 15 cm long cryogenic target has an apparent width of about 3.5 cm; 3-sigma cuts should remove essentially all the Al background rate while reducing the data rate less than 20%. This problem will be less severe at larger angles. The rates from the endcaps are low enough that they will not lead to a lower data acquisition rate for the data of interest. Estimates of the proton rates from the Al endcaps of the target, using the code EPC [11], indicate that these rates vary from about 100 Hz for the 0.8 GeV data down to 1 Hz for the 4.0 GeV data. Nonetheless, we plan to measure some empty target backgrounds if this information is not available from spectrometer development data.

Except for the addition of a focal plane polarimeter (FPP), the experimental technique and energy range are similar to that of Experiments NE8 and NE17 at SLAC as well as the Hall C proposal 89-12. (There is also a large overlap between the current collaboration and those experiments.) In fact, data were taken at SLAC during experiment NE8 [12] which directly address the proposed experimental technique. At SLAC, with the hydrogen target in place, the 1.6 GeV spectrometer was tuned for protons to look for the $H(\gamma, p)\pi^0$ reaction. Radiator in and radiator out data were taken for an electron energy of 1.2 GeV and a spectrometer angle of 42° . The $H(\gamma, p)\pi^0$ events were seen after subtraction of the radiator out data. The ep scattering rate was comparable with the $H(\gamma, p)\pi^0$ rate for these kinematics. The data from the SLAC experiments give confidence that the experimental technique, other than the use of the polarimeter, should be straightforward for the setup that we have proposed.

The FPP planned for Hall A is currently under construction by Rutgers University and the College of William & Mary. There is extensive experience measuring proton polarization with carbon FPP's, as is planned for Hall A, up to $T_p = 800\text{MeV}$ at Los Alamos and the other meson factories. There is excellent overlap (about 2 - 3% variations) between the calibrations of the various FPP's, leading to confidence that there should be no difficulty in operations at CEBAF up to 800 MeV kinetic energy. This range includes data points for 0.8 and 1.6 GeV photon energy.

Various of the Hall A polarimetry experiments require measurements of the

polarization for kinetic energies above 2 GeV. For these experiments, we plan to calibrate the FPP by measuring the $H(\vec{e}, e'\vec{p})$ reaction. The knowledge of magnetic and electric form factors of the proton up to $Q^2 = 4.5 (\text{GeV}/c)^2$, beam polarization, and spin transport will allow the FPP to be calibrated for proton energies up to 2.4 GeV with good precision. This calibration should in principle agree with that of the the POMME polarimeter [13] at SACLAY. POMME has now been calibrated to a kinetic energy of 2.4 GeV. This covers our proton energy range at 90°_{cm} , and all points except for 4.0 GeV photon energy at 45°_{cm} and 60°_{cm} . Given our precision requirements, it should be possible to simply import the POMME calibration for the current experiment. Note that even if there are systematic errors at the 5% level in the calibration, the resulting proton polarization will be little changed, e.g., from 0.20 to 0.19 or 0.21. In particular, since the analyzing power appears as a multiplicative factor in calculating the polarization from the measured asymmetry, it does not increase the uncertainty in determining the deviation of the measurement from 0.

Extension of the polarimeter calibration above this energy requires a continuation of the $H(\vec{e}, e'\vec{p})$ measurement to $Q^2 \sim 5.6 (\text{GeV}/c)^2$ and/or use of a liquid hydrogen analyzer in the spectrometer focal plane so that the carbon may be cross calibrated to known H analyzing powers. Each of these methods is time consuming, because of the small flux of protons for $Q^2 > 4 (\text{GeV}/c)^2$ and the large statistics needed to calibrate the polarimeter. At this stage, the Hall A FPP Working Group has not evaluated which method is preferred or whether the experimental accuracies required by the various polarimeter experiments require that both methods be used.

Commissioning the polarimeter also involves a set of calibration runs to examine the detector alignment and response. False asymmetries from the device can be checked with unpolarized e^-p elastic scattering, which should yield zero polarization. These checks can be performed parasitically, or at high data rates using unpolarized protons. The polarimeter design goal is to keep false asymmetries below the level of 0.005. With an analyzing power of about 0.2, this corresponds to a false polarization of <0.025 .

In the discussion above, we have ignored the issue of spin transport. For $p(\gamma, \vec{p})\pi^0$ the proton polarization will be normal to the reaction plane. The longitudinal and sideways components, P_l and P_s , are zero. As the proton is transported through the spectrometer, the spin will precess about the magnetic field into the longitudinal direction, with the net precession resulting mostly from the dipole magnets. The precession angle is given by $\chi = 1.79\omega\gamma$, where 1.79 is the numerical value of $g_p/2 - 1$, ω is the bend angle of the spectrometer, and $\gamma = E/m$ is the Lorentz factor. For much of the kinematic range of the

experiment, in particular for the higher energy points at 90_{cm}° , spin precession changes the direction of the proton polarization by close to 180° or 360° , so that the magnitude of the polarization is essentially as large at the focal plane as at the target.

Thus, the proton polarization in the detector stack will have both normal and longitudinal components. Only the transverse polarization components are measured in the FPP, through the spin-orbit contribution to proton scattering from carbon. With $P_s = 0$, the proton scatters in the carbon block of the FPP with an angular distribution shape $I_o(\Theta)[1 + P'_n A_c(\Theta) \cos(\phi)]$, where $I_o(\Theta)$ is the unpolarized angular distribution, P'_n is the transverse polarization in the focal plane, A_c is the analyzing power of carbon, and ϕ is the azimuthal angle. The useful range in scattering angle Θ is typically 5° to 20° , for which $A_c \approx 0.2$ near 1 GeV kinetic energy, and falls slowly with energy.

From consideration of the points discussed above, we believe this experiment is appropriate for early running at CEBAF. Technical demands from the experiment are slight. Only the Hall A spectrometers and the cryotarget are required. Particle identification, energy resolution, and angular precision requirements are all modest and well below the design requirements of the equipment. The only exception is the transverse position resolution at the target which is used to reduce the running time by removing the need for empty target subtractions. For this parameter, the design resolution of 1 mm is desirable. Power load on the cryotarget, 200 W, is modest. With respect to the polarimeter, we believe the precision of the calibration required is such that we could run the experiment before the FPP is calibrated onsite by the $p(\vec{e}, e'\vec{p})$ reaction. The major time dependence in FPP calibrations results from relative motions of the detectors, leading to false asymmetries, which are handled by recalibrating the detector alignment. If needed, corrections from a subsequent calibration could be applied to the data.

VI. TIME ESTIMATES

Count rates have been calculated under the following assumptions. The cross sections for the $H(\gamma, p)\pi^0$ reaction are extrapolated from 5 GeV data using the scaling laws for the kinematics proposed. We use a 15 cm (1.2 g/cm^2) liquid hydrogen target. The beam current varies between $0.1 \mu\text{A}$ at 0.8 GeV to $50 \mu\text{A}$ at 4 GeV. The photon flux is calculated for a 6% radiator. The HRS spectrometer has a solid angle of 7.0 msr, and is assumed to be 80% efficient at detecting particles. Polarimeter efficiency and analyzing power has been taken from the preliminary POMME data.

Statistical uncertainties have been determined from the following considerations. Systematic uncertainties on the polarization are about 0.025 from false asymmetries, 0.01 from the analyzing power calibration, and 0.01 from spin transport through the spectrometer, leading to a total systematic uncertainty of 0.03. Since the spin transport causes the polarization at the target and in the focal plane to be about equal in magnitude for much of our kinematics, these uncertainties also apply to the polarization at the target. We aim for a statistical uncertainty of about 0.05, which is larger but close to the systematic uncertainty. This number includes a contribution from subtraction of the unpolarized electrodisintegration background under the worst case assumption that the background rates equal the photodisintegration rates. Thus, the final uncertainties will generally be 0.05 statistical + 0.03 systematic.

The resulting time estimates are shown in Table 1. The total time request, including time for electrodisintegration measurements, is 48 hours, if the experiment can run in conjunction with experiment 89-019 which has been already approved for 18 days of running in Hall A. If the experiment cannot be run in conjunction with experiment 89-019, an additional two days of beam time will be necessary for detector checkout, tune-up and some additional background runs and radiator linearity checks. These estimated times include no contingency factor for accelerator or spectrometer operation; in particular, no time is requested for beam energy or angle changes, since the time required for these is uncertain. Also, we have assumed that the polarimeter will be aligned before the experiment starts.

The *Call for Proposals* for PAC 8 requests a table of time required at each beam energy. These times have been summarized for the production data in Table 2. Again, we have not included overhead in the times listed.

VII. COLLABORATION BACKGROUND AND RESPONSIBILITIES

Many members of the current collaboration were involved in the deuteron photodisintegration experiments NE8 and NE17 at SLAC. A significant fraction of the collaboration is also involved in the Hall C experiment (89-012) to measure the $d(\gamma, p)n$ cross section up to 4 GeV photon energy, and the Hall A experiment (89-019) to measure the photoproton polarization in the $d(\gamma, \vec{p})n$ reaction up to 2.8 GeV. That experiment has also been accepted into the Hall A collaboration. This experiment includes many of the individuals within Hall A responsible for developing the focal plane polarimeter (Rutgers, Georgia). It is anticipated that it will be presented to the Hall A Collaboration for approval prior to the PAC meeting. All major components of the equipment needed for this experiment are part of the standard package of equipment in Hall A, except for the radiator, which will be built by Rutgers.

VIII. REFERENCES

- [1] R. L. Anderson *et al.* Phys. Rev. D **14**, 679 (1976).
- [2] P. V. Landshoff and J. C. Polkinghorne, Phys. Lett. **44B**, 293 (1973).
- [3] C. E. Carlson, M. Chachkhunashvili, and F. Myhrer, Phys. Rev. D **46**, 2891 (1992).
- [4] E. A. Crosbie *et al.* Phys. Rev. D **23**, 600 (1981).
- [5] G. Farrar, S. Gottlieb, D. Sivers, and G. Thomas, Phys. Rev. D **20**, 202 (1979); S. J. Brodsky, C. E. Carlson, and H. Lipkin, Phys. Rev. D **20**, 2278 (1979).
- [6] see D. G. Crabb *et al.*, Phys. Rev. Lett. **65**, 3241 (1990), and references therein.
- [7] T.-S. H. Lee, private communication.
- [8] Discussions of scaling may be found in, e.g., S. J. Brodsky and G. R. Farrar, Phys. Rev. Lett. **31**, 1153 (1973); V. A. Mateev *et al.*, Lett. Nuovo Cimento **7**, 719 (1973); S. J. Brodsky and G. R. Farrar, Phys. Rev. D **11**, 1309 (1975).
- [9] Hall A Line of Sight Shielding, CEBAF Tech. Note TN-91-024, K. A. Aniol and V. Punjabi (1991); Low Energy Neutron Shielding for Hall A Detector Hut, K. A. Aniol, (1991), unpublished.
- [10] R. Roy Whitney, CEBAF Technical Note, draft (1993).
- [11] J. W. Lightbody Jr. and J. S. O'Connell, Comp. Phys. May 1988.
- [12] J. Napolitano *et al.*, Phys. Rev. Lett. **61**, 2530 (1988); S. J. Freedman *et al.*, Phys. Rev. **C48**, 1864 (1993); T. Y. Tung, Ph.D. dissertation, Northwestern University (1992).
- [13] C. Perdrisat, private communication. See also B. Bonin *et al.*, Nucl. Inst. Meth. **A288**, 379 (1990).
- [14] Data and references can be found in *Compilation of Pion Photoproduction Data*, D. Menze, W. Pfeil, and R. Wilcke, Physikalisches Institut der Universitat Bonn (1977).

XI. FIGURE CAPTIONS

Figure 1: Diagrams of pp scattering mechanisms. The asymptotic amplitude involves a single hard gluon exchange between the two nucleons. The Landshoff amplitude involves 3 independent hard gluon exchanges between the different quarks of the two nucleons. The asymptotic amplitude is short range – the quarks within each nucleon must be close together – and conserves quark and hadron helicities. Spatial separations between the quarks within each nucleon in the Landshoff amplitude allows nonzero orbital angular momenta, so that nucleon helicities may not be conserved, although quark helicities are.

Figure 2: Left panel: Cross sections [14] for $H(\gamma, \pi^+)$ at $\theta_{\text{cm}} = 90^\circ$. Right panel: Cross sections [14] for $H(\gamma, p)\pi^0$ at $\theta_{\text{cm}} = 90^\circ$. The dashed curves are arbitrarily normalized and have a fall-off of s^{-7} .

Figure 3: The top panel shows the ratio $R = s^{10}d\sigma/dt$ vs. $\ln(s)$. The lower panel gives the A_{nn} data vs. $\ln(s)$. The curve is from Ref. [3] and includes the effects of independent quark scattering (Landshoff).

Figure 4: pp analyzing powers, from Crabb *et al.* [6].

Figure 5: Upper panel: A comparison of a calculation of the meson-exchange model with the $H(\gamma, \vec{p})\pi^0$ polarization measurements at $\theta_{\text{cm}} = 90^\circ$. Lower panel: Calculated angular distributions for $H(\gamma, \vec{p})\pi^0$ polarization at four energies.

Table 1 Kinematics and time estimates for the $H(\gamma, \vec{p})\pi^0$ reaction. The time requested determines the uncertainty to 0.05 (statistical). Cross sections and rates for $H(\gamma, p)\pi^0$ are evaluated at the photon energy given, which is 50 MeV less than the beam energy.

E_γ GeV	θ_{lab} deg	p_p GeV/c	$d\sigma/d\Omega$ nb/sr	I_e μA	$H(\gamma, p)\pi^0$ rate Hz	ep rate Hz	time hours	θ_{process} deg
$\theta_{\text{cm}} = 45^\circ$								
0.75	20.1	0.929	3.6E5	0.1	3800	55	0.5	113
1.55	17.9	1.702	3.2E4	0.5	874	22	0.5	167
2.35	16.1	2.426	6.2E3	1.0	112	4.2	1.2	223
3.15	14.8	3.132	1.8E3	10.0	24	1.3	11.5	281
3.95	13.7	3.829	660	10.0	7.1	0.5	1.5	338
subtotal							15.2	
$\theta_{\text{cm}} = 60^\circ$								
0.75	27.0	0.862	3.6E4	0.1	1521	81	0.5	109
1.55	24.2	1.561	3.2E3	1.0	342	34	0.5	156
2.35	22.0	2.208	614	2.0	43	7.0	0.8	206
3.15	20.2	2.835	174	50.0	9.1	2.2	4.0	256
3.95	18.8	3.453	63	50.0	2.6	0.9	2.0	307
subtotal							7.8	
$\theta_{\text{cm}} = 90^\circ$								
0.75	41.2	0.686	1.4E4	0.5	1419	582	0.5	100
1.55	37.9	1.205	1.2E3	1.0	124	131	0.5	131
2.35	34.9	1.666	209	2.0	15	32	1.0	164
3.15	32.5	2.104	56	10.0	2.9	11	1.8	198
3.95	30.5	2.530	20	50.0	0.8	4.5	6.0	232
subtotal							9.8	
beam total							32.8	
overhead ¹							15.0	
TOTAL							47.8	

¹Overhead assumes that experiment runs in conjunction with approved experiment 89-019

Table 2 Time requested for production data at each beam energy. Overhead has not been included.

E_{e^-} incident GeV	time needed hours
0.8	1.5
1.6	1.5
2.4	3.0
3.2	17.3
4.0	9.5

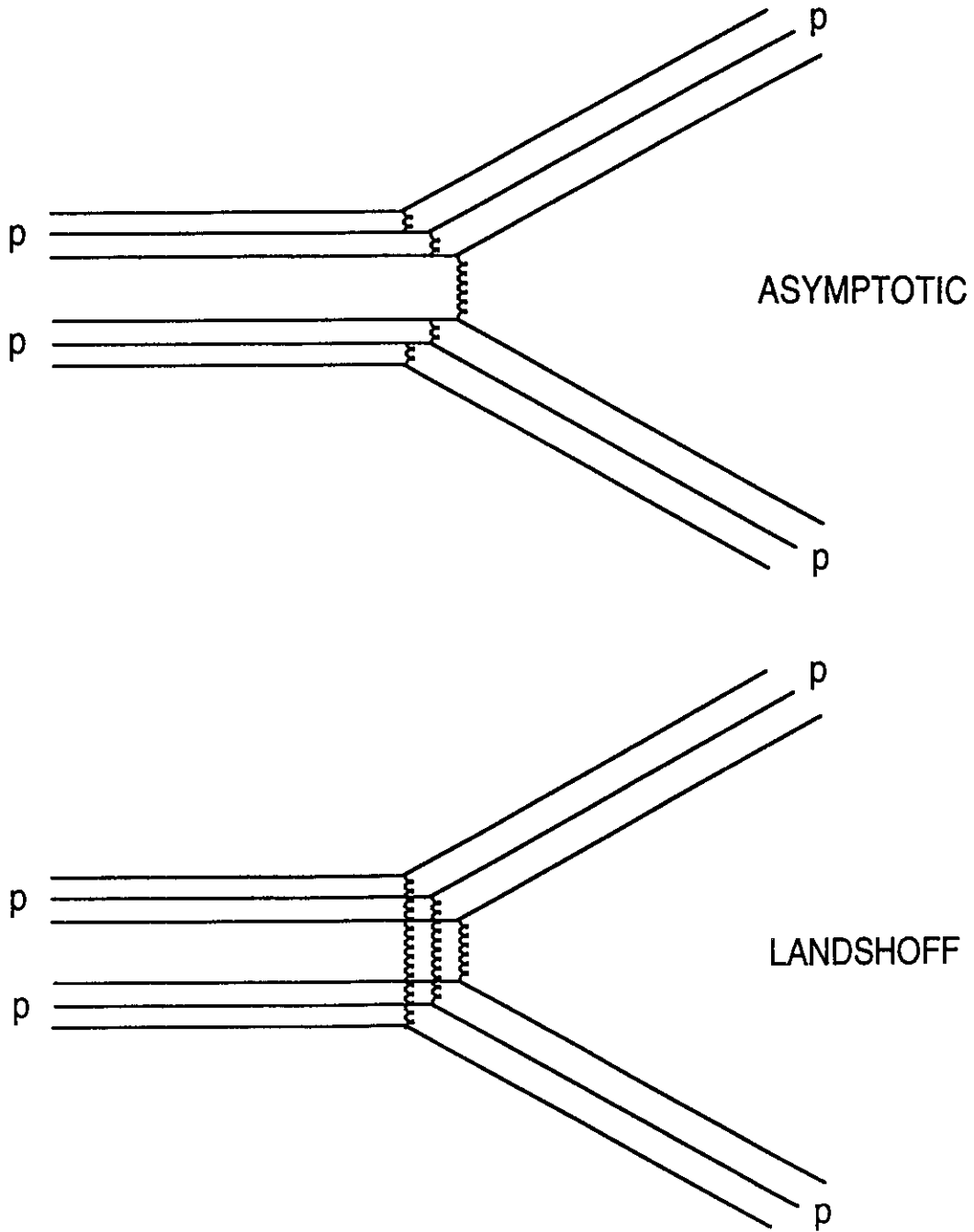


Fig. 1

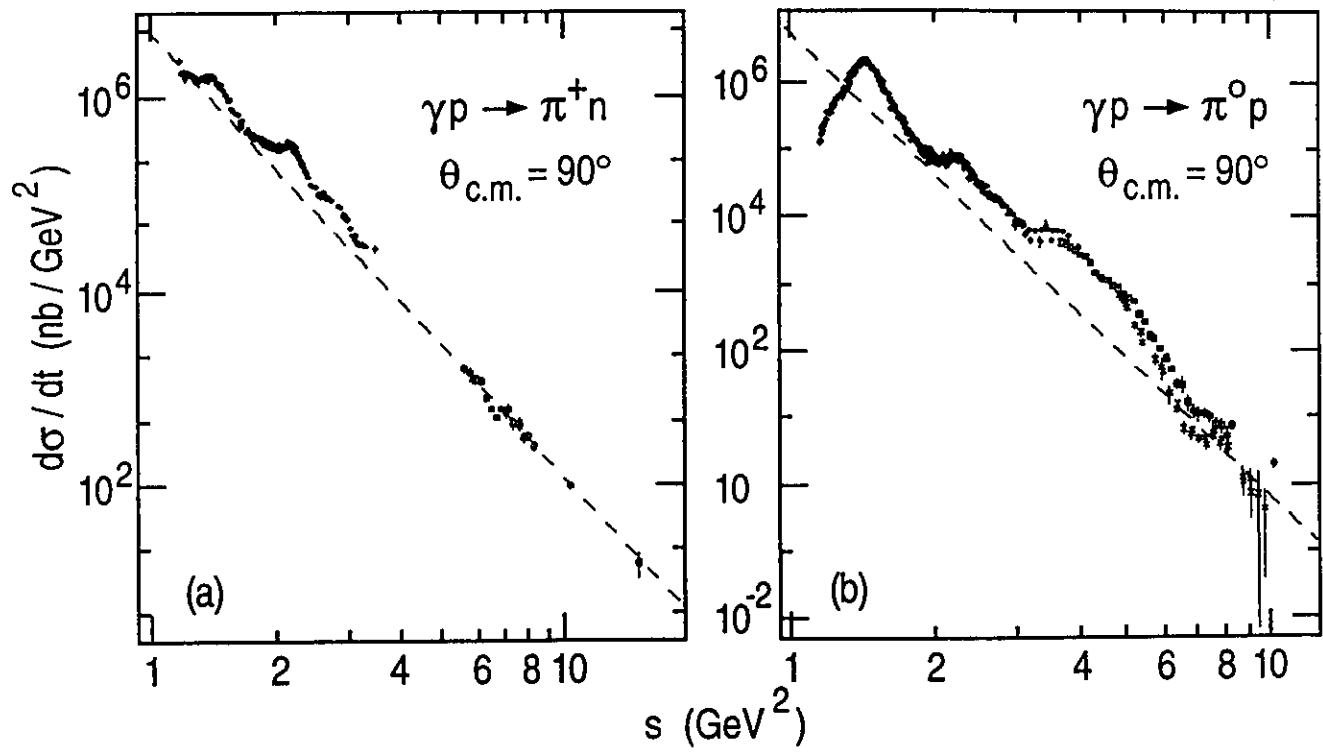


Fig. 2

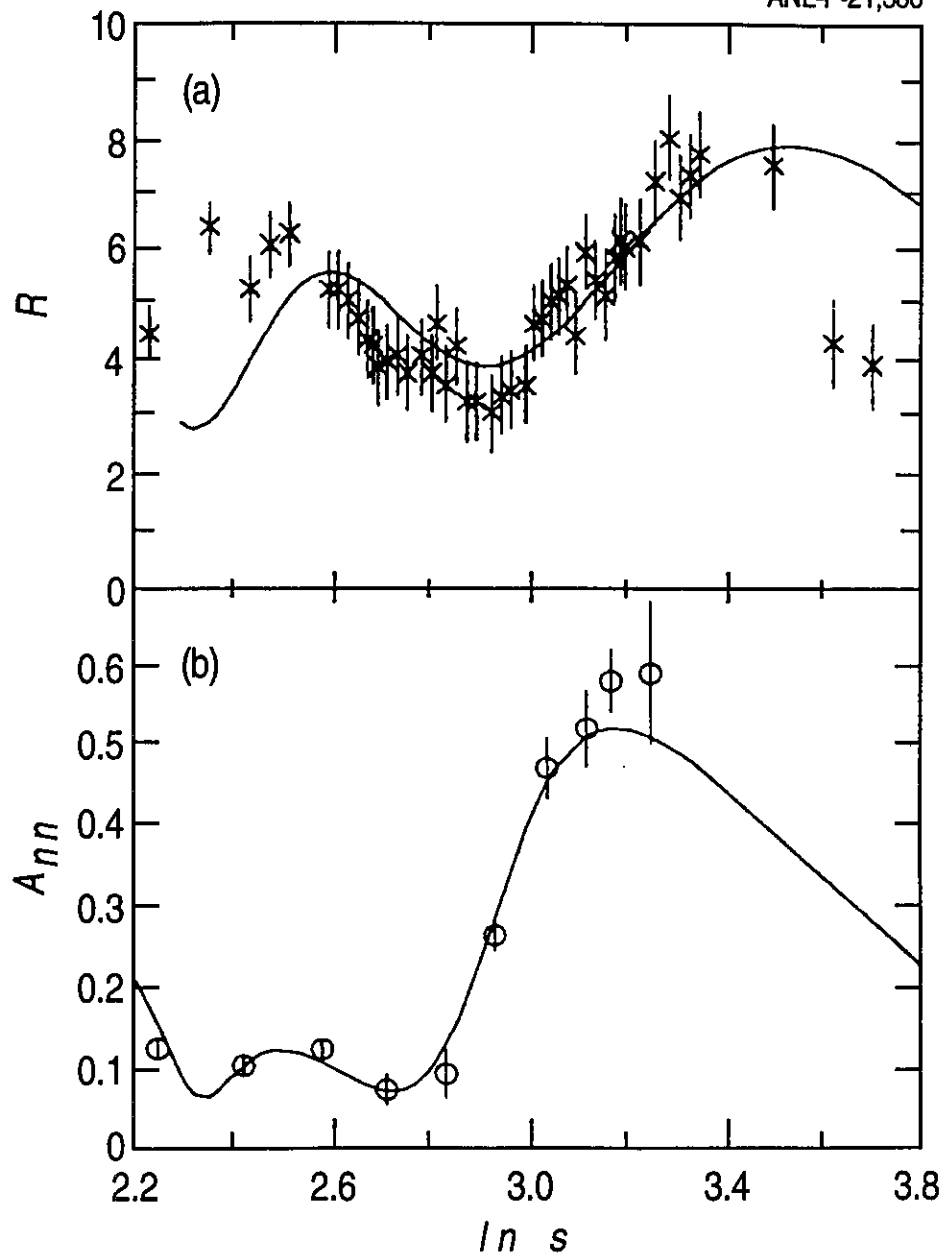


Fig. 3

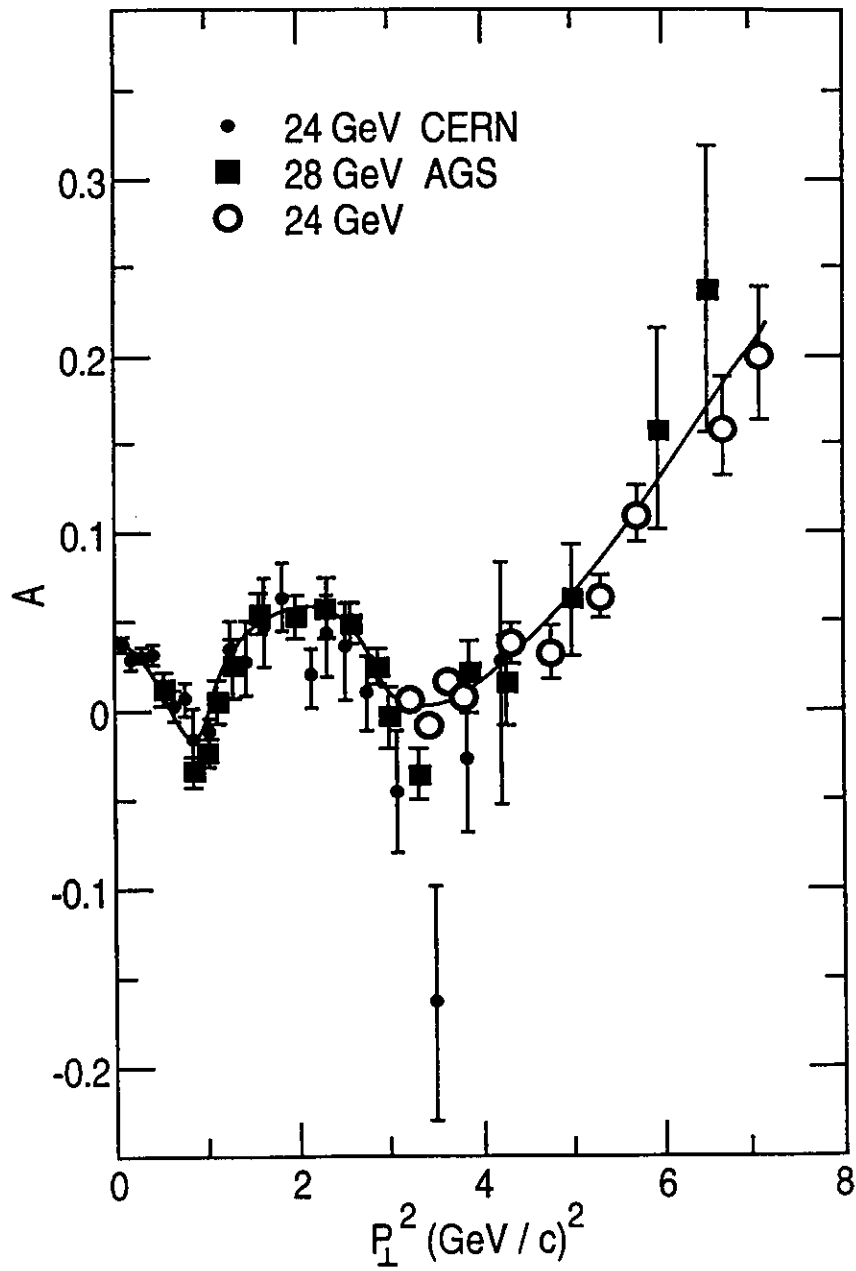


Fig. 4

$\rho(\alpha, p)\pi^0$ at $\theta_{cm} = 90^\circ$

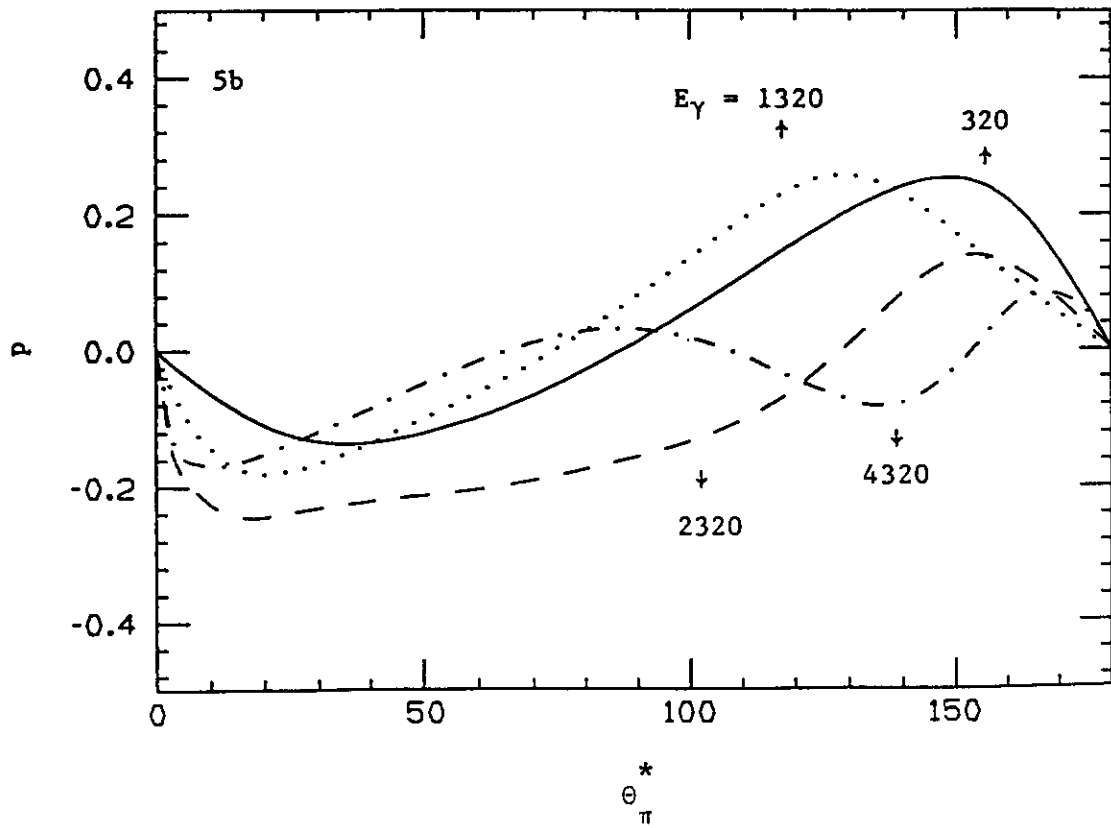
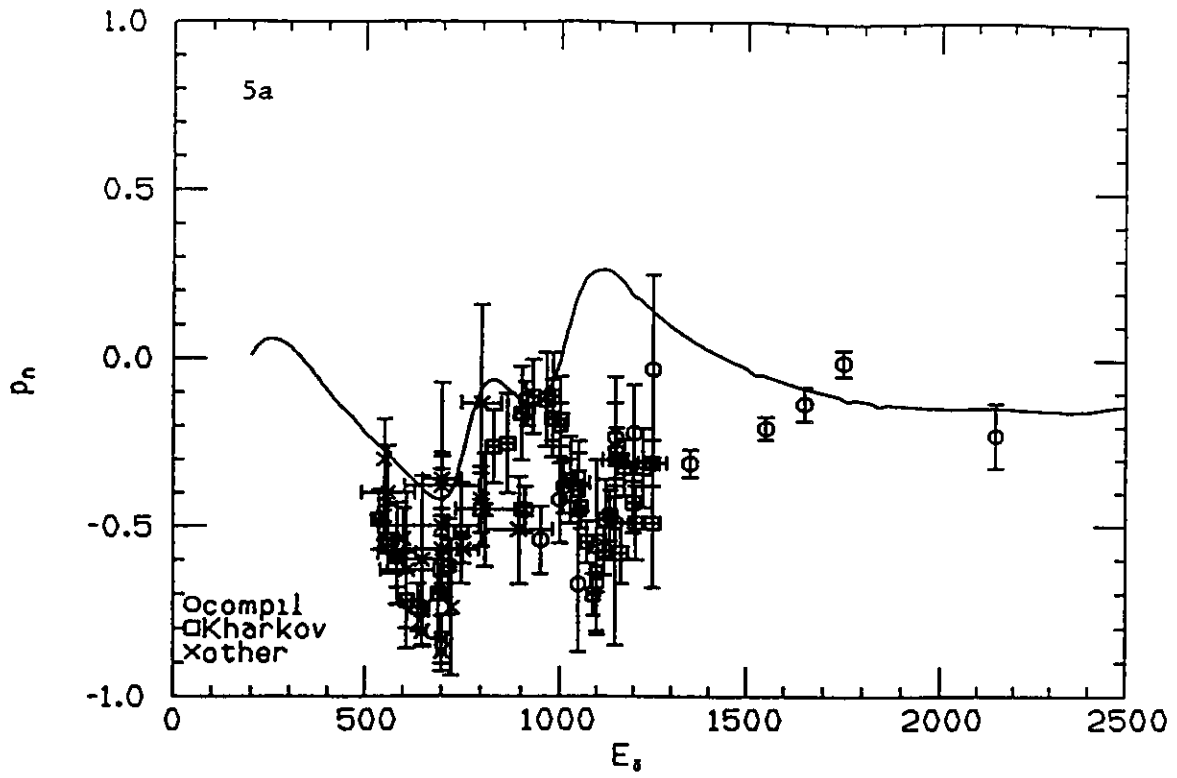


Fig. 5